理冲消癥颗粒通过上调ANT3介导的线粒体凋亡增强小鼠卵巢癌移植瘤对顺铂的敏感性

陈一锣[1],马 民[1],苏 燃[1],朱寅宾[1],冯 晴[1],罗嘉丽[1],冯伟峰[2],颜显欣[1]
[1]暨南大学中医学院,广东 广州 510632;[2]暨南大学附属第一医院,广东 广州 510630

摘要:目的 探讨理冲消癥颗粒通过调控ANT3介导的线粒体凋亡通路增敏顺铂治疗卵巢癌的分子机制。**方法** LC-MS检测理冲消癥颗粒入血成分。采用皮下异种移植瘤模型,将BALB/c-nud小鼠随机分为3组(8只/组):Tumor组(仅接种肿瘤)、DDP组(每周腹腔注射1次0.1 mL的5 mg/kg的顺铂)、DDP_LCXZ组(在顺铂基础上按照15 g·kg^{-1}·d^{-1}灌胃0.2 mL的理冲消癥颗粒)。在实验过程中动态监测肿瘤体积、质量及小鼠体质量,并用HE染色观察肿瘤和肾脏的病理学变化。同时,采用RNA-seq筛选差异基因并行KEGG分析,电镜用于观察线粒体结构变化,Western blotting检测线粒体凋亡相关蛋白的表达。**结果** LC-MS共检测出218个成分为理冲消癥颗粒的入血成分;与Tumor组比较,DDP组与DDP_LCXZ联合用药组的肿瘤体积分别减少60.3%和72.6%(P<0.01)。转录组学结果显示,ANT3在DDP组与DDP_LCXZ联合用药组中的表达水平较对照组上调(P<0.05)。分子对接后发现理冲消癥颗粒的主要活性成分与ANT3的结合能均<-6 kcal mol。电镜显示,与Tumor组相比,DDP组肿瘤细胞线粒体肿胀及外膜损伤程度增加,DDP+LCXZ组该现象更为明显。Western blotting结果显示,DDP组和DDP+LCXZ组中BAX、ANT3、cleaved-caspase-3、cleaved-caspase-9表达水平升高,而BCL-2表达水平降低(P<0.05)。**结论** LCXZ通过上调ANT3,促进线粒体功能失衡并激活凋亡信号,从而增强顺铂对卵巢癌的抑瘤效应。
关键词:理冲消癥颗粒;腺苷酸转位酶3;线粒体凋亡;化疗增敏;卵巢癌

Lichong Xiaozheng Granules enhances cisplatin sensitivity of ovarian cancer xenografts in rats by regulating adenine nucleotide translocator 3-mediated mitochondrial apoptosis

CHEN Yiliu[1], MA Min[1], SU Ran[1], ZHU Yinbin[1], FENG Qing[1], LUO Jiali[1], FENG Weifeng[2], YAN Xianxin[1]
[1]College of Traditional Chinese Medicine, Jinan University,Guangzhou 510632,China; [2]First Affiliated Hospital,Jinan University,Guangzhou 510630,China

Abstract: Objective To investigate the molecular mechanism by which *Lichong Xiaozheng* Granules (LCXZ) sensitize ovarian cancer to cisplatin (DDP) treatment. **Methods** LC-MS analysis was used to identify the blood components of LCXZ after its administration in mice *via* gavage. In a BALB/c mouse model bearing subcutaneous ovarian cancer xenografts, the effects of daily gavage of distilled water (control group), intraperitoneal injection of DDP (5 mg/kg) once a week, or both DDP injection and daily LCXZK gavage (15 g/kg) on tumor growth were evaluated. Histopathological changes in the xenografts and kidneys were assessed with HE staining. RNA-seq was performed to identify the differentially expressed genes followed by KEGG pathway analysis. The changes in mitochondrial ultrastructure and expressions of mitochondrial apoptosis-related were examined with transmission electron microscopy and Western blotting. **Results** A total of 218 blood-borne components of LCXZ were detected by LC-MS. In the tumor-bearing mice, treatments with DDP and DDP combined with LCXZ redcued the tumor volume by 60.3% and 72.6% compared with that in the control group, respectively. Transcriptomic analysis revealed significantly upregulated ANT3 expression in both the two treatment groups. Molecular docking indicated that the main active components of LCXZ were capable of binding to adenine nucleotide translocator 3 (ANT3) with binding energies below -6 kcal/mol. Transmission electron microscopy showed obvious mitochondrial swelling and outer-membrane damage in the tumor cells in DDP-treated mice, and these changes were more pronounced in the combined treatment group. The expression levels of BAX, ANT3, cleaved caspase-3 and cleaved caspase-9 were increased, whereas BCL-2 expression was decreased significantly in the tumor cells in both the DDP and DDP+LCXZ groups. **Conclusion** LCXZ enhances the therapeutic efficacy of cisplatin against ovarian cancer xenografts in mice by promoting mitochondrial dysfunction and activating apoptotic signaling pathways via upregulating ANT3.
Keywords: *Lichong Xiaozheng* Granules; adenine nucleotide translocator 3; mitochondrial apoptosis; chemo-sensitization; ovarian cancer

收稿日期:2025-06-26
基金项目:国家自然科学基金(82074430);广东省基础与应用基础研究基金项目(2024A1515011722);广州市科技计划项目(2024B03J1261,2024B03J1262);广东省中医药局科研项目(20241062);广东省基础与应用基础研究基金省企联合基金-面上项目(2022A1515220105)
Supported by National Natural Science Foundation of China (82074430).
作者简介:陈一锣,在读博士研究生,E-mail:cyl9708@163.com;马 民,教授,博士生导师,E-mail: tmamin@jnu.edu.cn;陈一锣、马 民共同为第一作者
通信作者:冯伟峰,副主任医师,硕士生导师,E-mail: fwf2000ok@sina.com;颜显欣,副教授,硕士生导师,E-mail: 871655006@qq.com

卵巢癌(OC)是全球女性肿瘤相关死亡率最高的恶性肿瘤之一,最新的统计显示其年发病和死亡病例分别超过30万和20万例,5年生存率不足45%[1]。在我国,OC发病率持续攀升,约70%的患者在确诊时已属中晚期[1];目前手术联合含铂化疗仍为一线方案,其中顺铂凭借显著疗效被广泛应用。然而,约30%的患者存在原发耐药,70%的初治敏感者亦常在6~12个月内出现获得性耐药,加之顺铂相关肾毒性等不良反应,共同限制了其长期的临床应用[3, 4]。研究表明,p53功能缺失以及线

粒体通透性转变孔(mPTP)长期关闭所维持的跨膜电位(ΔΨm)稳态等因素是肿瘤细胞对顺铂治疗敏感性降低的关键机制[4]。尽管PARP抑制剂、血管生成抑制剂和新一代铂类药物联合顺铂治疗已显示一定效果,但受限于对特定基因背景(如BRCA1/2突变)的依赖、毒副反应的累积以及高昂的费用,其大规模临床推广仍面临挑战[6, 8]。

在线粒体介导的抗凋亡网络中,腺苷酸转位酶3(ANT3)是mPTP复合体的关键亚基,具有"阀门"功能[9]。在对顺铂敏感的肿瘤细胞中,ANT3的高表达可诱导mPTP持续或周期性开放,放大线粒体依赖性的凋亡信号[10, 11];而在对顺铂耐受或敏感性降低的肿瘤细胞中,ANT3的下调导致mPTP的长期闭合,显著抬高凋亡阈值[12]。尽管体外研究已证实ANT3与顺铂敏感性密切相关,其体内表达动态、上游调控网络及针对性干预策略仍缺乏系统阐释,亟待进一步研究。

近年来,具有"多成分—多靶点"特点的中药在化疗增敏和减毒方面展现独特优势:柴胡桂枝汤可下调MDR1的表达减少化疗药物的外排,槲皮素通过抑制ERCC1/XPA通路抑制DNA的修复,丹参酚酸B通过促进mPTP开放恢复线粒体凋亡[13, 14]。然而,现有研究大多将注意力聚焦于复方中的单体成分,缺乏对"多成分协同—多靶点共调"整体效应的系统阐释[15];成分复杂、靶点繁多且药代动力学特征不明,使复方研究难以形成可重复、可量化的证据链,从而制约了中医药成果的临床转化与国际影响力的提升。

中医认为OC属"癥瘕"范畴,治疗强调"攻补兼施、祛瘀扶正"[16]。理冲消癥颗粒(LCXZK)由桂枝茯苓丸、理冲丸加减化裁而成,临床应用已显示一定抑瘤和缓解化疗毒性的潜力,但其作用机制尚未明晰[17]。本研究通过构建裸鼠卵巢癌移植瘤模型,首次整合理冲消癥颗粒的入血成分分析、转录组学分析与分子对接,构建"入血成分-靶点-通路"网络,系统解析LCXZK的活性成分谱及其对ANT3的调控作用,研究发现LCXZK可通过上调ANT3促进mPTP的持续开放从而激活线粒体凋亡信号,协同顺铂抑制卵巢癌的进展,为临床上理冲消癥颗粒协调顺铂治疗卵巢癌提供实验室依据。

1 材料和方法

1.1 实验动物

从北京华阜康生物科技有限公司购得24只4~6周龄的雌性BALB/c-nud裸鼠,并在暨南大学SPF实验动物管理中心饲养。动物实验经暨南大学动物伦理委员会批准(伦理批号:IACUC-20240408-01),并严格按照批准的方案执行。

1.2 动物分组与给药

团队的前期研究发现[17],LCXZK灌胃给药7.5~15 g·kg^{-1}·d^{-1}的给药剂量存在潜在的增敏作用,综合考虑单药效、动物耐受,我们最终选择LCXZK中剂量进入联合用药方案。LCXZK中剂量为15 g·kg^{-1}·d^{-1},由临床用量9 g·kg^{-1}·d^{-1}经体表面积换算而确定。将24只小鼠随机分为3组(8只/组):肿瘤对照(Tumor)组、顺铂治疗(DDP)组、顺铂联合理冲消癥颗粒治疗(DDP_LCXZ)。小鼠适应性喂养7 d后,将1×10^{6}的卵巢癌细胞系-Hey皮下种植至小鼠右侧腋下。当平均肿瘤体积达到80~100 mm^{3}时开始治疗:Tumor组小鼠每日纯水灌胃200 μL,每周腹腔注射1次0.1 mL生理盐水;DDP组小鼠每日纯水灌胃200 μL,每周腹腔注射1次0.1 mL的5 mg/kg浓度的顺铂;DDP-LCXZ组小鼠每日灌胃0.2 mL的15 g·kg^{-1}·d^{-1}浓度的LCXZK,每周腹腔注射1次0.1 mL的5 mg/kg浓度的顺铂。

1.3 所用试剂

顺铂(HY-17394)(MEDCHEMEXPRESS LLC)、黄芪配方颗粒、党参配方颗粒、三棱配方颗粒、莪术配方颗粒、当归配方颗粒、水蛭配方颗粒、白芍配方颗粒、桃仁配方颗粒、丹皮配方颗粒、茯苓配方颗粒、桂枝配方颗粒(广东一方制药有限公司),甲醇(A452-4)、乙腈(A998-4)、甲酸(A117-50)(赛默飞世尔科技有限公司)。β-Tubulin(2128T;1∶1000, Western blotting)、Cleaved Caspase-9(9509T;1∶1000, Western blotting)、Bcl-2(3498T;1∶1000, Western blotting)、Bax(2772T;1∶1000, Western blotting)抗体(Cell Signaling Technology, Inc);Cleaved-Caspase-3(MB0711S;1∶1000, Western blotting)抗体(上海艾比玛特医药科技有限公司);ANT3(GB112438-100;1∶800, Western blotting)、ki67(GB111499-50, 1∶500, IHC),HRP标记的山羊抗兔IgG(GB23303, 1∶5000, Western blotting),HE染液(G1005-100ML)(武汉赛维尔生物科技有限公司);RIPA裂解液(WB3100)(苏州新赛美生物科技有限公司)。

1.4 HE染色

小鼠肿瘤组织取材固定,经过脱水、透明、石蜡包埋、切片后依次进行苏木精染色、伊红染色,最后经脱水、透明并封片,显微镜下观察拍照。

1.5 入血成分分析

采用液相色谱-质谱联用技术(LC-MS/MS)分析理冲消癥颗粒的入血成分。理冲消癥颗粒组血清样品经甲醇-乙腈提取后,通过UPLC HSS T3色谱柱分离,流动相为0.1%甲酸水溶液和0.1%甲酸乙腈,梯度洗脱。质谱参数设置为正负离子模式,扫描范围m/z 100~1200,分辨率70 000/17 500。同时按上述流程检测理冲消癥颗粒原药成分及肿瘤对照组血清成分作为对照,数据使用Progenesis QI 3.0处理,结合数据库检索、保留时间、质量误差及标准库MS^{2}一致性确认化合物。并按以下原则鉴定入血成分及次级代谢产物:满足理冲消癥颗

粒原药成分有峰、理冲消癥颗粒组血清有峰、理冲消癥颗粒组血清组/肿瘤对照组血清的峰面积值≥10；代谢产物：满足理冲消癥颗粒原药成分无峰、理冲消癥颗粒组血清组/有峰、理冲消癥颗粒组血清组/肿瘤对照组血清的峰面积值大于等于≥10。

1.6 转录组测序

小鼠新鲜肿瘤组织立即置于液氮中冷冻保存，干冰运输，转录组学测序及后续的相关数据分析均由上海欧易生物医药科技有限公司负责完成。差异基因筛选阈值：$|\log_2FC|\geq1$、FDR<0.05（比较组：DDP *vs* Tumor；DDP+LCXZ *vs* DDP）。功能富集采用KEGG（q<0.25，*p*.adj<0.05）评估通路变化。

1.7 分子对接

从TCMSP数据库（https://tcmsp-e.com）中下载芍药苷、L-苦杏仁苷、松二糖、苯甲酰芍药苷的mol2结构文件，再从PDB数据库（https://www.rcsb.org）中下载ANT3的PDB结构文件。运用PyMOL软件对受体蛋白进行去水、加氢和移除原始配体等操作。利用Auto Dock Tools 1.5.6软件将芍药苷、L-苦杏仁苷、松二糖、苯甲酰芍药苷与ANT3进行分子对接。最后，通过PyMOL软件和Discovery Studio 4.5 Client软件展示分子对接结果。

1.8 免疫印迹实验

取各组小鼠的肿瘤组织，RIPA裂解液提取总蛋白。参照团队先前的实验研究进行电泳、转膜、封闭、孵育二抗、显影[18]。

1.9 统计学分析

样本量通过G*Power 3.1.9.6进行计算。基于末次瘤积数据，折算得到效应量f=0.94；在检验水准α=0.05（双侧）和检验效能1−β=0.80的设定下，每组最低需7只动物可满足检验效能的要求。利用SPSS 13.0进行数据分析，计量资料以均数±标准差表示，多组间比较先进行方差齐性检验，方差齐者采用单因素方差分析，两两比较采用LSD检验，方差不齐者采用Dunnett's T_3检验，*P*<0.05为差异有统计学意义。

2 结果

2.1 理冲消癥颗粒的入血成分分析

HPLC-UV指纹图谱显示，理冲消癥颗粒在210 nm下以皂苷等极性成分为主峰（图1A），而在254 nm下则突出含苯环和共轭双键的芳香类成分的响应峰（图1B）。通过对采集的正、负离子模式下理冲消癥颗粒及含药血清高分辨质谱数据进行解析，共鉴定或推导218个入血成分，具体化合物详细碎片的鉴定信息（表1）。代表性解析路径如下：以芍药苷为例，正离子模式检测到母离子峰m/z 479.2，MS^2主要碎片包括m/z 449.1（脱去CH_2O）、m/z 327.1（去苯甲酰基）与m/z 165.1（苯甲酰基碎片），与标准品一致（图1C）。

表1 理冲消癥颗粒中鉴定出的含量Top 20的入血化合物的信息

Tab.1 Information on the top 20 compounds of *Lichong Xiaozheng* Granules (LCXZ) detected in medicated mouse serum

No.	Mass-to-charge ratio (m/z)	Formula	Mass Error (ppm)	Retention time (min)
M0001	387.1132	C12H22O11	-3.69	0.89
M0002	170.0210	C7H6O5	-3.02	1.87
M0003	329.0869	C14H18O9	-2.67	3.13
M0004	183.0293	C8H8O5	-3.03	3.90
M0005	356.1097	C16H20O9	-2.96	4.04
M0006	496.1569	C23H28O12	-2.36	4.15
M0007	457.1572	C20H27NO11	-2.76	4.29
M0008	431.1910	C19H30O8	-3.31	4.51
M0009	481.1692	C23H28O11	-2.65	4.62
M0010	295.1044	C14H17NO6	-4.10	4.67
M0011	480.1618	C23H28O11	-2.89	4.71
M0012	446.1200	C22H22O10	-2.88	4.88
M0013	428.1671	C20H28O10	-2.70	4.97
M0014	580.2141	C28H36O13	-2.51	5.12
M0015	433.1130	C21H22O10	-2.46	5.25
M0016	463.1221	C22H22O11	-3.07	5.26
M0017	441.1756	C20H28O8	-2.57	5.41
M0018	507.1491	C23H26O10	-3.62	5.58
M0019	161.0593	C10H10O3	-2.29	5.71
M0020	507.1493	C23H26O10	-3.22	5.90

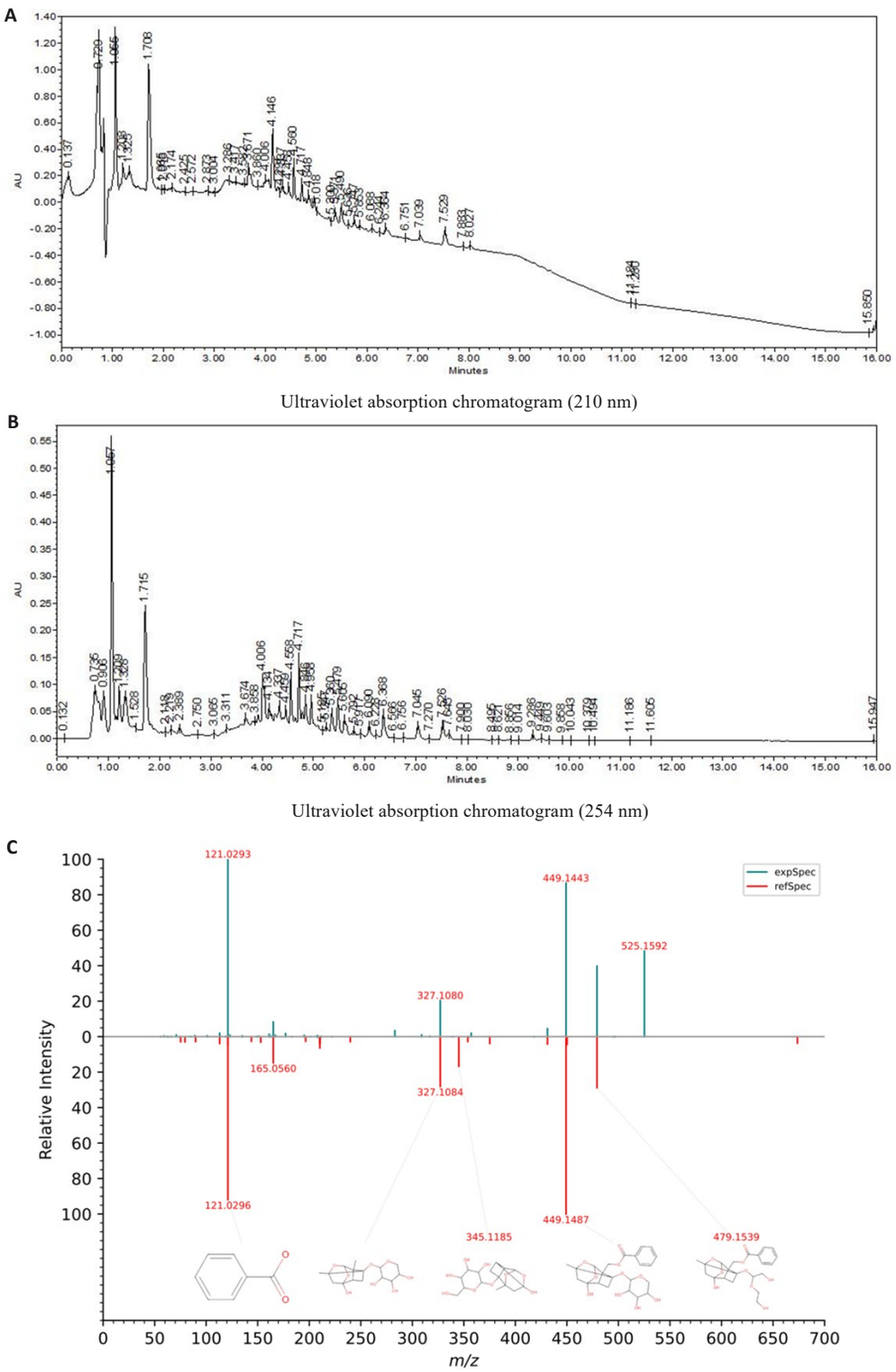

图1 理冲消癥颗粒的 HPLC-UV 指纹图谱及代表性成分质谱解析

Fig. 1 HPLC-UV fingerprints and mass spectrometric analysis of *Lichong Xiaozheng* Granules (LCXZ). **A**, **B**: HPLC-UV fingerprint of LCXZ at 210 nm and 254 nm, respectively. **C**: High-resolution mass spectrometric fragmentation pathway of paeoniflorin.

2.2 理冲消癥颗粒协同顺铂抑制卵巢癌的增殖

小鼠瘤积的变化及Ki67染色的结果表明理冲消癥颗粒能够协同顺铂抑制卵巢癌的增殖(图2A、B、E)。小鼠肿瘤的瘤质量的变化结果显示:与肿瘤对照组相比,DDP组肿瘤生长受到显著抑制,抑制率为60.3%,理冲消癥颗粒能够协同顺铂进一步抑制小鼠肿瘤的增殖,抑制率为72.6%(P<0.05,图2C)。HE染色的结果也显示,理冲消癥颗粒协同顺铂治疗后,小鼠肿瘤组织细胞间隙增宽、局灶坏死增加,肿瘤增殖活性受到进一步的抑制(图2D)。

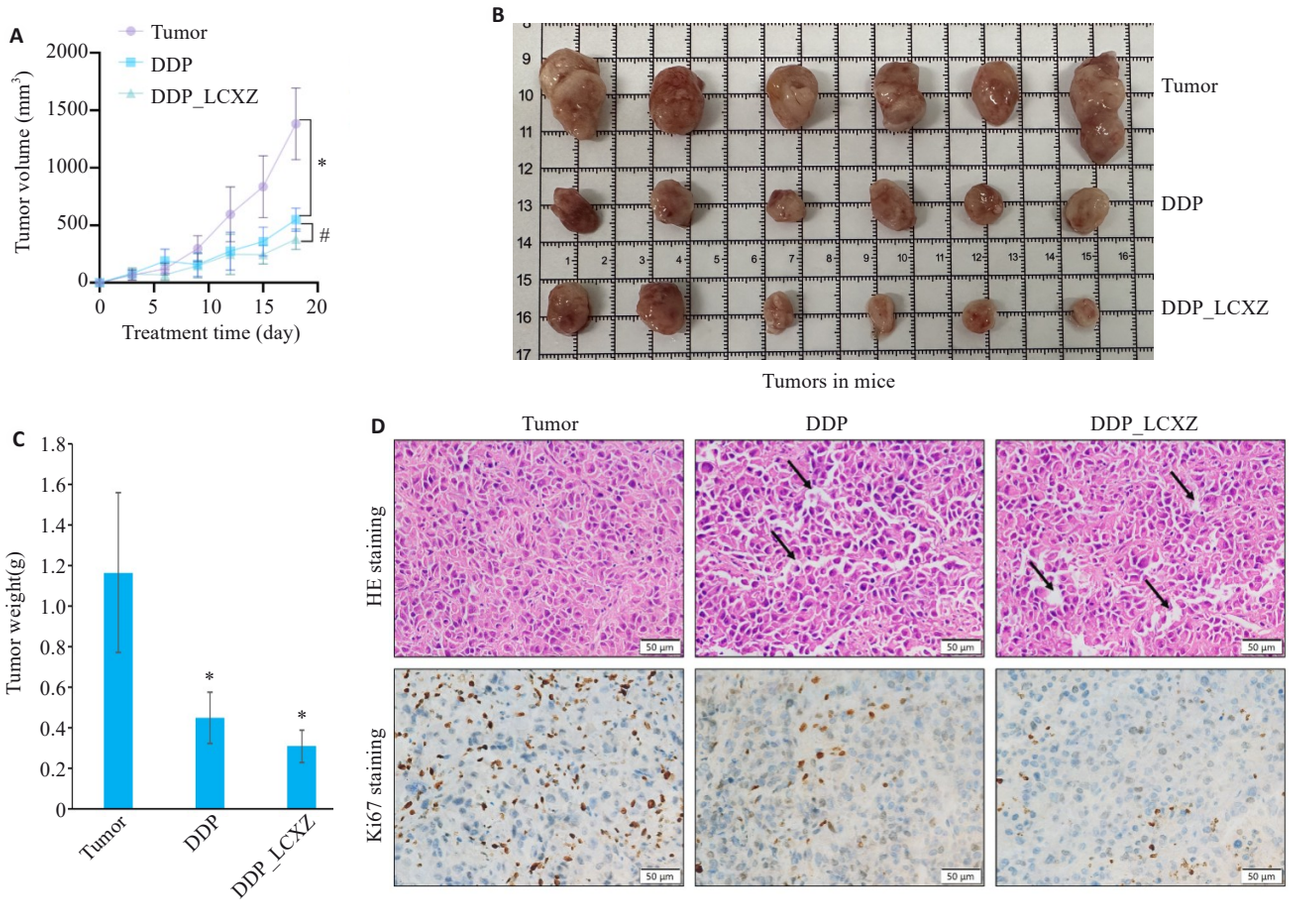

图2 理冲消癥颗粒协同顺铂抑制卵巢癌的增殖

Fig.2 LCXZ synergizes with cisplatin to inhibit ovarian cancer proliferation in nude mice. **A**: Measurement of tumor volume in the mice. **B**: Gross observation of the dissected tumors. **C**: Measurement of tumor weight. **D:** HE/Ki67 staining of the tumors, Arrows indicate widened intercellular spaces (Original magnification: ×400). **P*<0.05 *vs* Tumor group, #*P*<0.05 *vs* DDP group (*n*=8).

2.3 理冲消癥颗粒缓解顺铂的毒性作用

小鼠体质量的变化(图3A)、脾脏形态的改变(图3B)、肾脏HE染色结果(图3C)及肾脏组织SOD检测(图3D)结果共同表明,顺铂治疗可引起显著的系统性毒性反应,包括体质量下降、脾脏萎缩及肾小管损伤等;而联合理冲消癥颗粒后,这些毒性均得到一定程度的缓解。肾脏组织SOD检测结果(图3D)显示:与Tumor组相比,DDP组小鼠的肾脏组织SOD含量下降,而联合理冲消癥颗粒治疗小鼠肾脏组织的SOD含量得到回升,与肾脏HE染色的结果趋势一致。LCXZ具有良好的减毒保护作用,尤其在肾脏结构保护和免疫器官维持方面表现出积极效果。

2.4 理冲消癥颗粒协同顺铂治疗靶点的转录组学分析

转录组学的PCA图结果表明,PC1+PC2共提供了62.99%的解释度,各组间的区分明显(图4A)。差异表达基因火山图的结果显示:与肿瘤对照组相比,DDP组中有186个基因表达发生显著变化,其中80个基因表达上调,106个基因表达下调(图4B);与肿瘤对照组相比,DDP+LCXZ组中共有166个基因表达发生显著变化,其中93个基因表达上调,73个基因表达下调(图4C);与DDP组相比,DDP+LCXZ组中有88个基因表达发生显著变化,其中72个基因表达上调,16个基因表达下调(图4D)。3组间的差异基因韦恩图结果显示,3组间共表达的差异基因有2个,分别是SKIL、ANT3,其中ANT3显示出更大的差异倍数,因此我们将ANT3确定为优先候选靶点(图4E)。

2.5 理冲消癥颗粒协同顺铂治疗靶点的KEGG富集分析

KEGG富集结果显示:顺铂较肿瘤对照显著关联凋亡、ABC转运体和氧化磷酸化等通路(图5A);在顺铂基础上联合理冲消癥颗粒,可进一步富集坏死性凋亡、VEGF/cGMP-PKG/MAPK等信号(图5B);与顺铂单用相比,联合用药特异性增强铁死亡、ECM-受体互作、PI3K-Akt等通路(图5C),提示LCXZ可能通过诱导铁死亡并协同调控血管生成与细胞-基质互作等多通路强化顺铂的抗肿瘤效应。

2.6 分子对接分析

选取TCM均值(峰面积的比值%)大于5%的中药单体作为主要入血成分:芍药苷(图6A)、L-苦杏仁苷(图6B)、松二糖(图6C)、苯甲酰芍药苷(图6D)分别

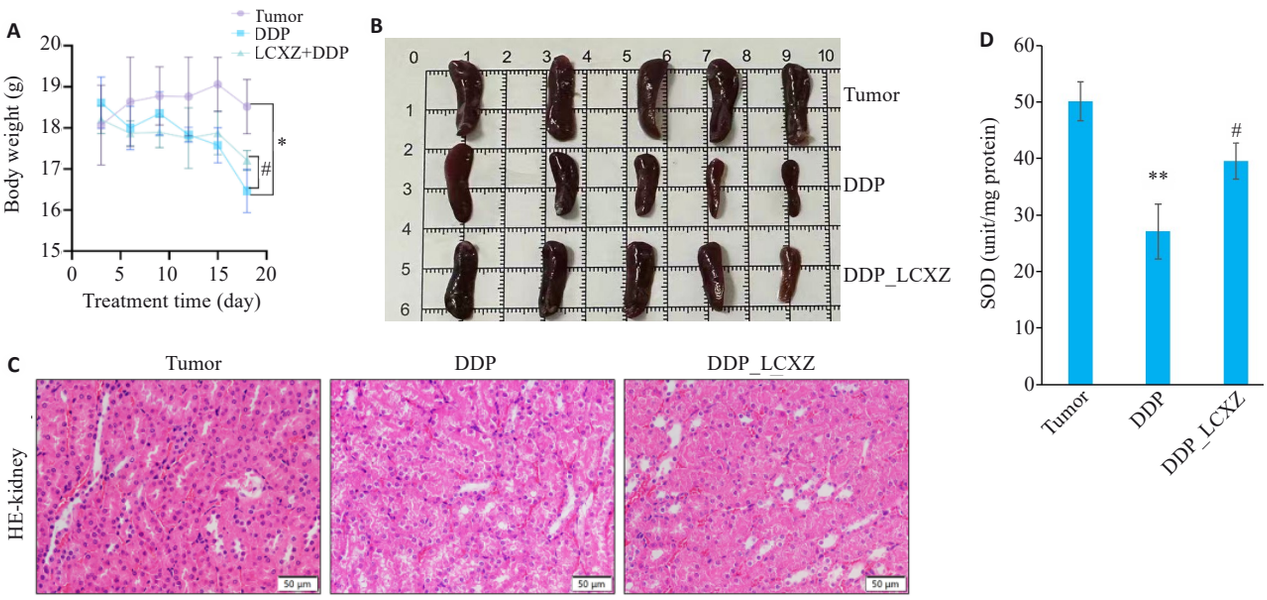

图3 理冲消癥颗粒缓解顺铂的毒性作用

Fig.3 LCXZ alleviates the toxic effect of cisplatin. **A**: Body weight changes of the tumor-bearing mice. **B**: Gross observation of the spleen of the mice. **C**: HE staining of renal tissues of the mice (×400). **D**: SOD content in the kidneys of the mice. **P*<0.05, ***P*<0.01 *vs* Tumor group; #*P*<0.05 *vs* DDP group (*n*=8).

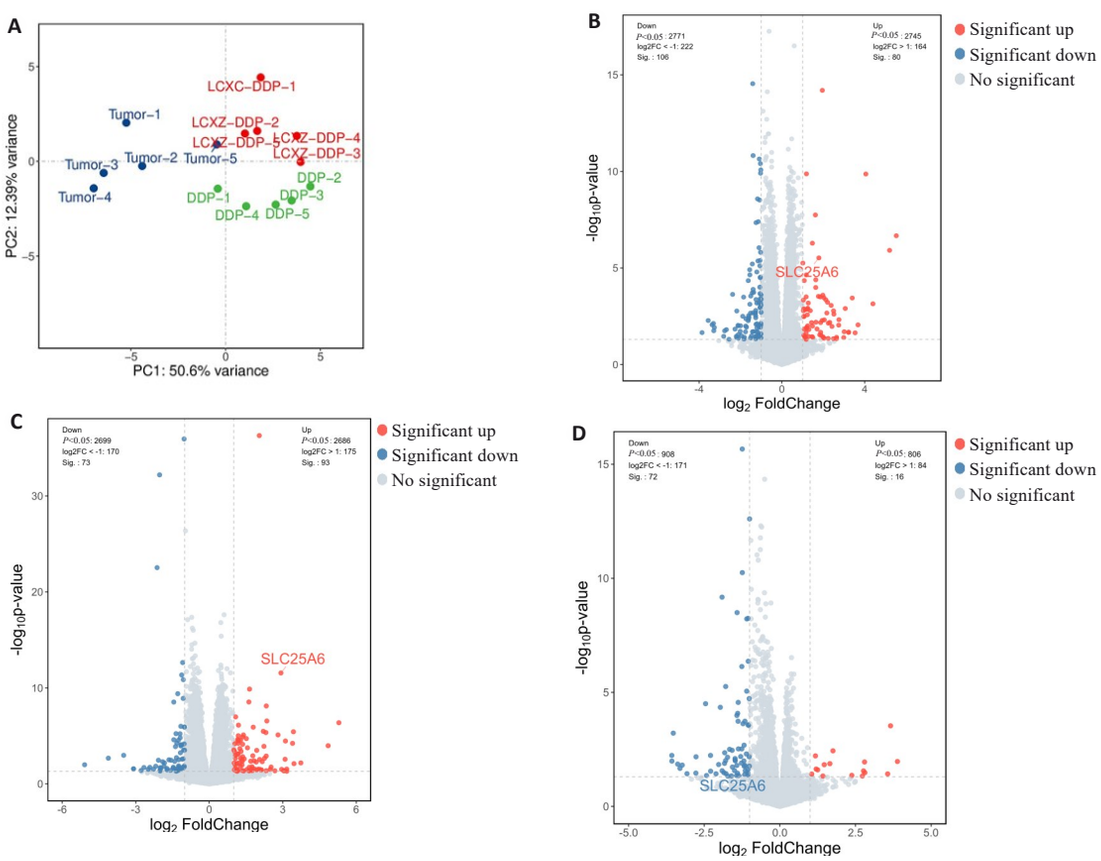

图4 理冲消癥颗粒协同顺铂治疗靶点的转录组学分析

Fig.4 Transcriptomic analysis of therapeutic targets of LCXZ combined with cisplatin. **A**: Principal component analysis. **B**: Volcano plot of the differential genes of DDP *vs* Tumor. **C**: Volcano plot of the differential genes of DDP_LCXZ *vs* Tumor. **D**: Volcano plot of the differential genes of DDP_LCXZ *vs* DDP. **E**: Venn diagram of the differential genes.

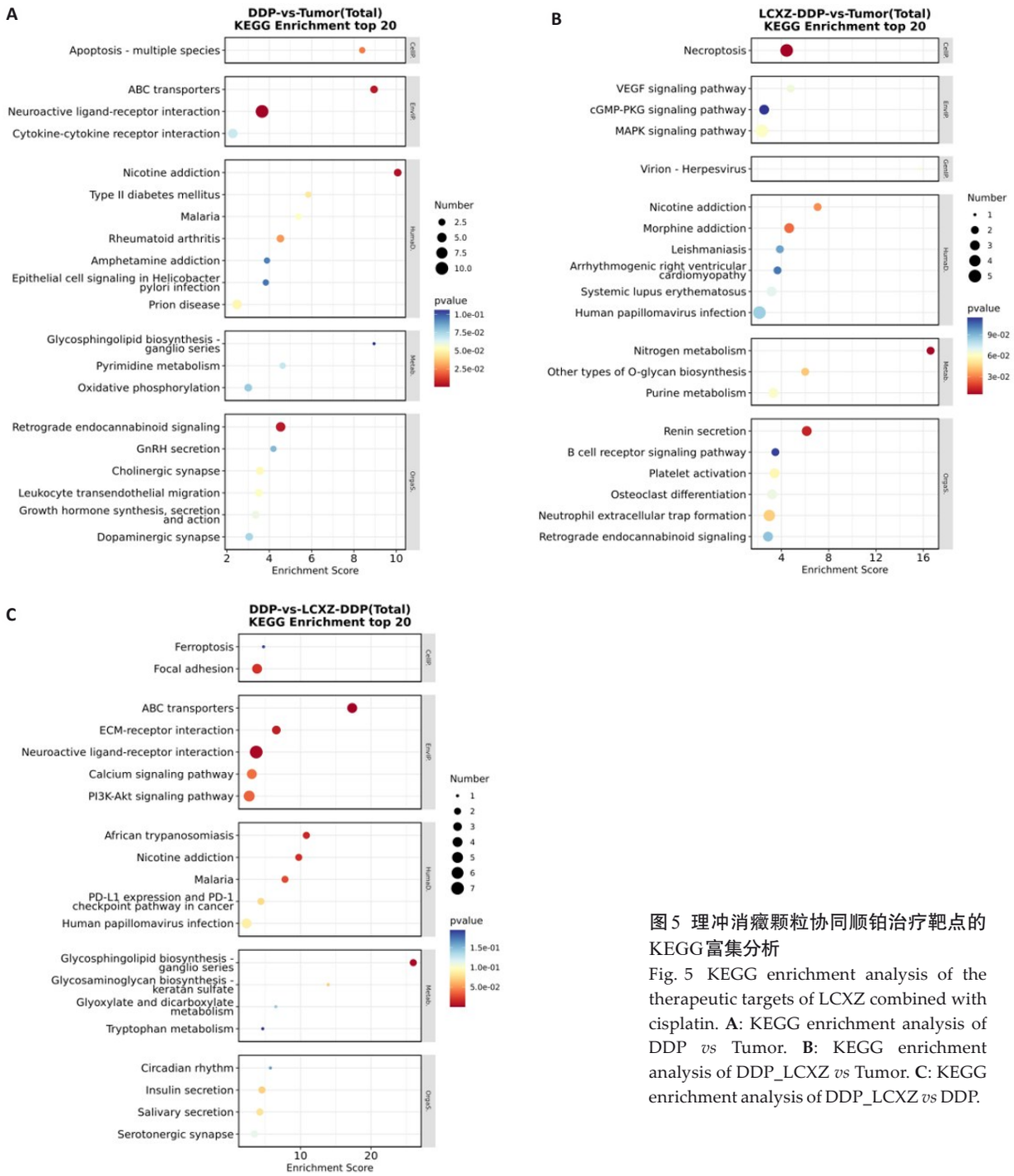

图5 理冲消癥颗粒协同顺铂治疗靶点的KEGG富集分析

Fig. 5 KEGG enrichment analysis of the therapeutic targets of LCXZ combined with cisplatin. **A**: KEGG enrichment analysis of DDP *vs* Tumor. **B**: KEGG enrichment analysis of DDP_LCXZ *vs* Tumor. **C**: KEGG enrichment analysis of DDP_LCXZ *vs* DDP.

与ANT3进行分子对接分析，受体-配体的结合能均<-6 kcal/mol。

2.7 理冲消癥颗粒协同顺铂导致肿瘤细胞线粒体孔过度开放

电镜结果显示，顺铂治疗后线粒体外膜出现局部的裂解，线粒体高度肿胀，部分膜间隙变宽，理冲消癥颗粒协同顺铂治疗后这一趋势得到进一步的扩大，呈现出与线粒体通透性转换孔过度开放相符的形态学特征。(图7)。

2.8 理冲消癥颗粒介导的线粒体凋亡通路增敏顺铂

Western blotting结果显示，与肿瘤对照组相比，理冲消癥颗粒联合顺铂处理后，肿瘤组织中ANT3、BAX、cleaved caspase-3、cleaved caspase-9的蛋白表达水平升高，而BCL-2的蛋白表达水平降低，差异具有统计学意义(P<0.05，P<0.01，图8A~F)。

3 讨论

卵巢癌是全球女性肿瘤相关死亡的首位原因[19]。顺铂虽为一线方案，却因显著的肾毒性和免疫抑制而受剂量限制[20, 21]；此外，约70%的患者在6~12个月内出现获得性耐药，导致复发率高、预后差[22, 23]。

中医认为卵巢癌属于“癥瘕”的范畴，病机以气滞血

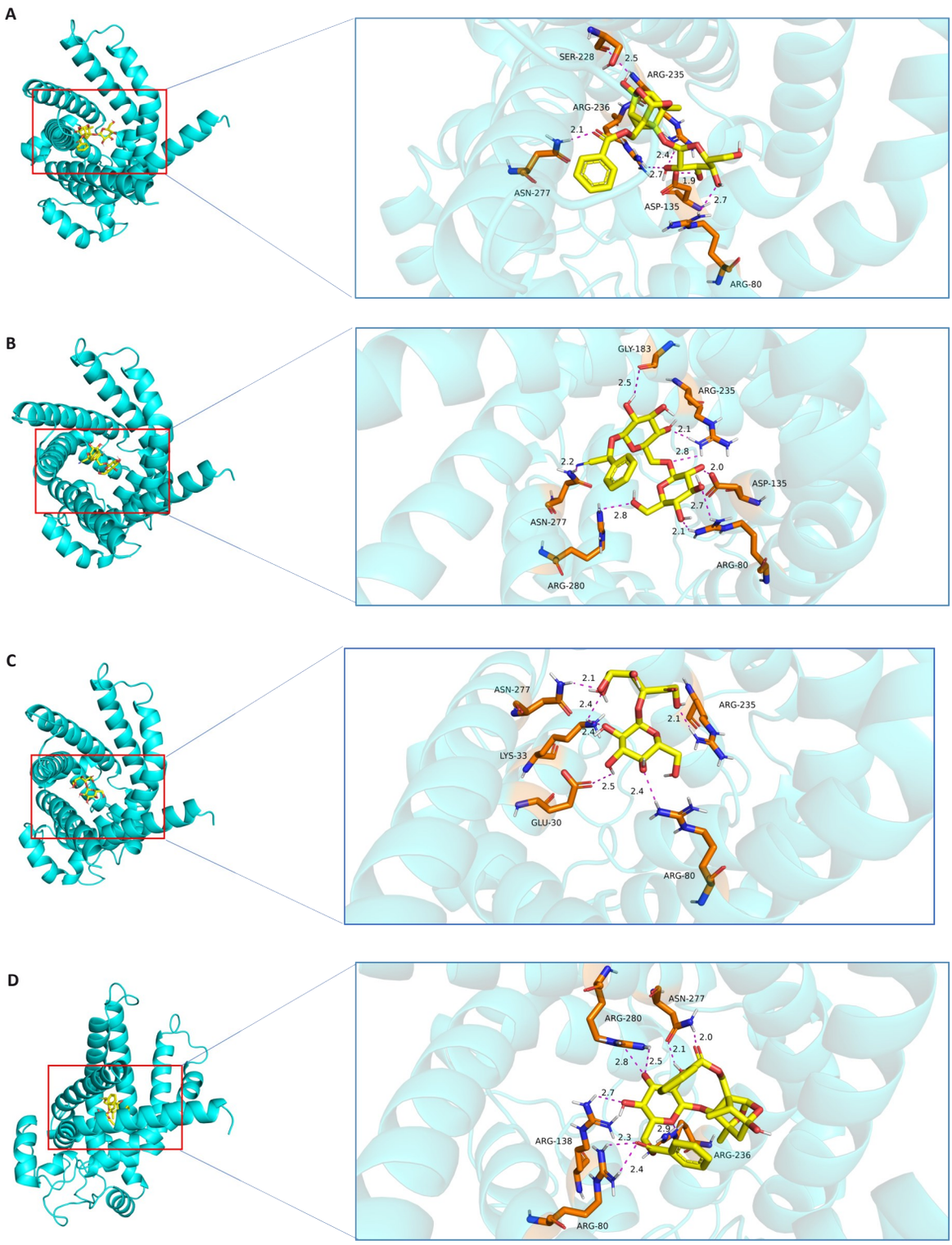

图6 理冲消癥颗粒主要成分的分子对接

Fig. 6 Molecular docking of the main constituents of LCXZ . **A**: Paeoniflorin-ANT3 docking. **B**: L-amygdalin-ANT3 docking. **C**: Turanose-ANT3 docking. **D**: Benzoyl paeoniflorin-ANT3 docking.

瘀、痰湿瘀毒互结为核心[24]。中药配方颗粒是在中医药理论指导下，由单味中药饮片经水提、分离、浓缩、干燥、制粒而成，具有疗效确切、不需煎煮、卫生安全等优势[25]。理冲消癥颗粒（LCXZK）由白芍、三棱、莪术等药组成，突出“活血化瘀、软坚散结、扶正解毒”之功，已在临床显示增效减的潜力。

我们首先通过HPLC-MS共鉴定出包括芍药苷、L-苦杏仁苷、松二糖、苯甲酰芍药苷在内的218个入血成分，为阐释理冲消癥颗粒的多靶活性提供了物质基础。为了进一步明晰理冲消癥颗粒协同顺铂抑制肿瘤的效果及机制，我们构建了卵巢癌细胞系-Hey的皮下移植瘤小鼠模型。研究结果发现，与单用DDP相比，

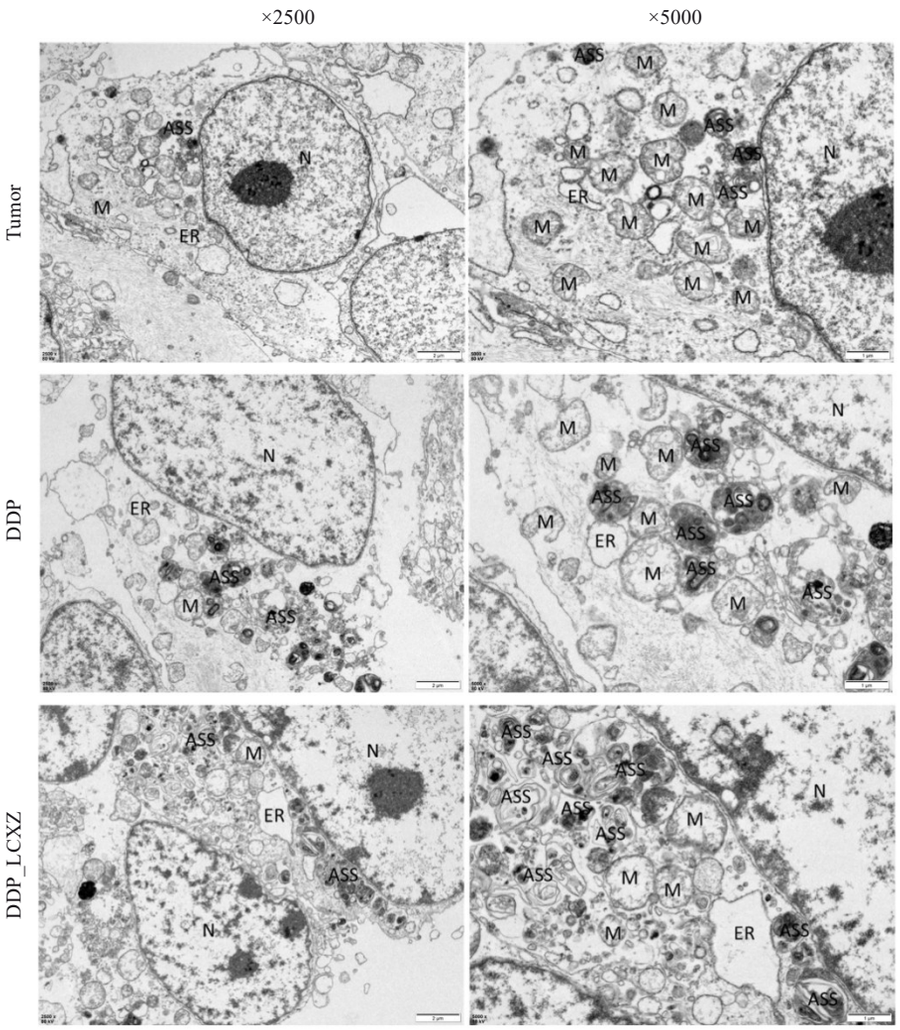

图7 理冲消癥颗粒协同顺铂导致肿瘤细胞线粒体孔过度开放

Fig.7 LCXZ combined with cisplatin causes excessive opening of the mitochondrial pores in the tumor cells. (Left: scale bar=2 μm; Right: scale bar=1 μm. Labels: N: nucleus; M: mitochondria; ER:endoplasmic reticulum; ASS: autophagolysosomal structure).

DDP_LCXZ显著降低小鼠的瘤积及瘤重,且进一步扩大抑瘤优势。同时,小鼠体质量、脾脏指数及肾小管病理损伤均得到明显改善,提示LCXZ能有够效缓解顺铂的毒性。转录组学分析表明,顺铂主要激活凋亡、氧化磷酸化和ABC转运体通路;在联合LCXZ后,坏死性凋亡、VEGF/cGMP-PKG/MAPK通路进一步富集,并特异性增强铁死亡、ECM-受体互作和PI3K-Akt信号通路的活性。这说明LCXZK可以通过多通路重塑肿瘤代谢与微环境,从而协同顺铂发挥更强的抗肿瘤效果。

进一步的差异基因筛选锁定了线粒体通透性转换孔(mPTP)的关键蛋白ANT3。ANT3位于内线粒体膜,是ADP/ATP交换的核心载体,也是mPTP的骨架蛋[26]。其过度表达或构象激活可诱导mPTP持续开放,引发线粒体膜电位丧失、细胞色素c释放并激活caspase-9/3级联反应,最终诱导细胞凋亡[27, 28]。结合前期研究中的多组学证据表明[17],LCXZK可能通过脂代谢重编程、ROS应激等通路改变肿瘤细胞的线粒体稳态,从而激活ANT3诱导卵巢癌细胞凋亡的进一步发生。分子对接研究表明,LCXZ的主要入血成分与ANT3的结合能均低于-6 kcal/mol,提示这些成分可能通过直接结合ANT3,促进其构象变化,进而诱导mPTP过度开放[29, 30],LCXZK是否能够直接靶向激活ANT3从而诱导细胞凋亡仍需要结合SPR等手段进一步验证。电镜观察显示,联合用药组的线粒体出现高度肿胀和嵴崩解,符合mPTP过度开放的特征[31, 32]。Western blotting结果进一步验证了联合用药组中ANT3上调、BCL-2下调的变化,同时观察到BAX的易位及caspase-9/3级联的激活。最终,这些变化共同触发了典型的线粒体途径凋亡[33]。

综上所述,LCXZ能够通过激活ANT3,诱导mPTP失控性开放,显著增强顺铂诱导的线粒体凋亡,从而提高顺铂的抗肿瘤效果。这一研究不仅揭示了LCXZ在卵巢癌治疗中的增效减毒机制,也为中药复方的多靶点抗肿瘤作用提供了分子证据。未来研究可进一步探索LCXZ中各活性成分对ANT3的调控机制,并在临床试

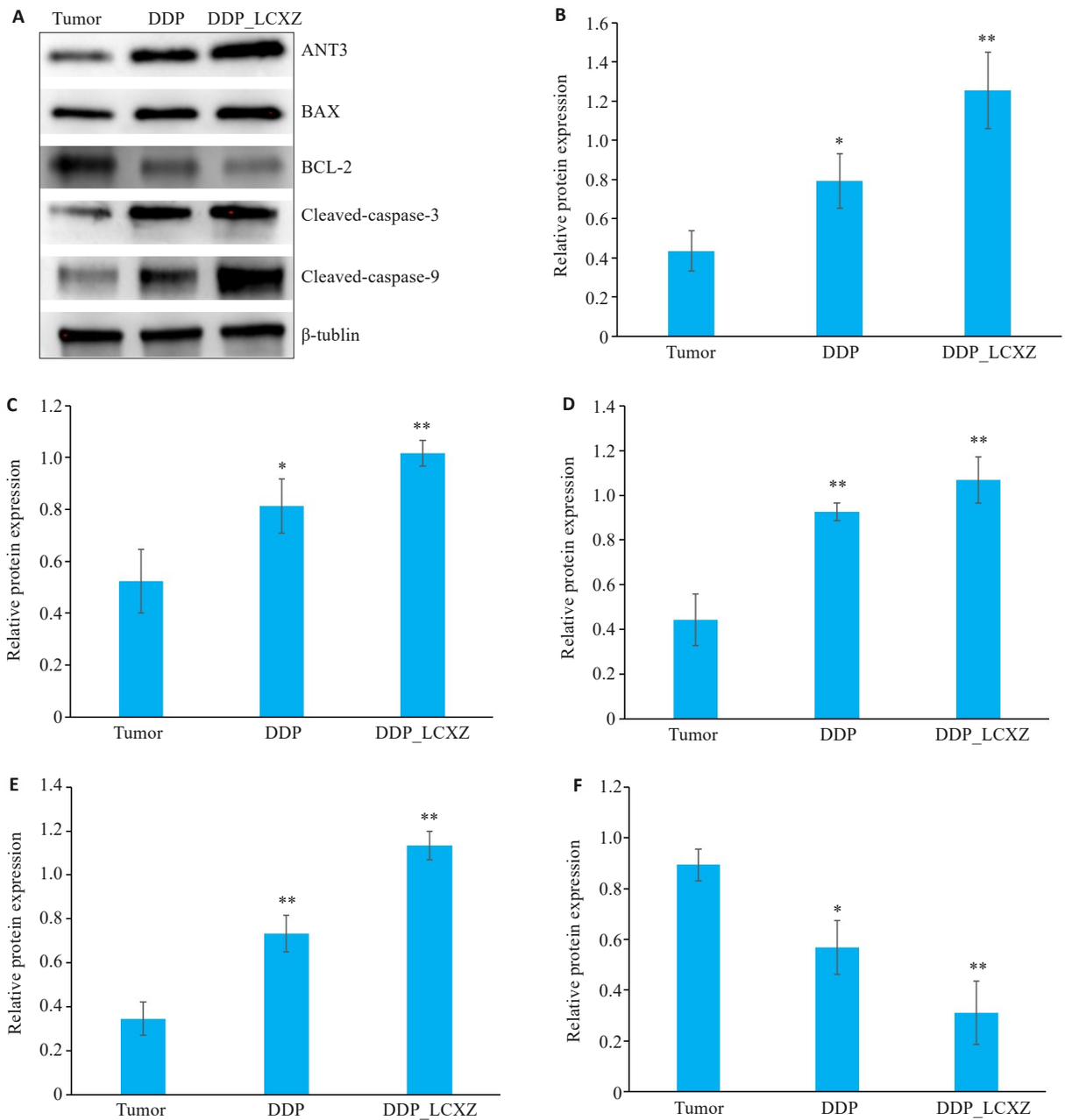

图8 理冲消癥颗粒介导的线粒体凋亡通路增敏顺铂

Fig. 8 LCXZ -mediated mitochondrial apoptosis pathway sensitizes cisplatin. **A**: Representitative protein bands in Westen blotting. **B-F**: Relative protein expression levels of ANT3, BAX, cleaved caspase-3, cleaved caspase-9 and BCL-2, respectively. **P*<0.05, ***P*<0.01 *vs* Tumor group (*n*=3).

验中验证其安全性和有效性，为开发新型卵巢癌治疗方案提供理论依据和支持。

Declaration of interests: The authors declare no competing interests.

参考文献：

[1] Sung H, Ferlay J, Siegel RL, et al. Global cancer statistics 2020: GLOBOCAN estimates of incidence and mortality worldwide for 36 cancers in 185 countries[J]. CA Cancer J Clin, 2021, 71(3): 209-49.

[2] Chen WQ, Zheng RS, Baade PD, et al. Cancer statistics in China, 2015[J]. CA A Cancer J Clinicians, 2016, 66(2): 115-32.

[3] Chen ZW, Shan JJ, Chen M, et al. Targeting GPX4 to induce ferroptosis overcomes chemoresistance mediated by the PAX8-AS1/GPX4 axis in intrahepatic cholangiocarcinoma[J]. Adv Sci (Weinh), 2025, 12(30): e01042.

[4] He ZK, Lian ZY, Wu JN, et al. PFKFB3 confers cisplatin resistance in gastric cancer by inhibiting ferroptosis through SLC7A11/xCT dephosphorylation[J]. Int Immunopharmacol, 2025, 159: 114914.

[5] Dasari S, Tchounwou PB. Cisplatin in cancer therapy: molecular mechanisms of action[J]. Eur J Pharmacol, 2014, 740: 364-78.

[6] Dibitetto D, Widmer CA, Rottenberg S. PARPi, BRCA, and gaps: controversies and future research[J]. Trends Cancer, 2024, 10(9): 857-69.

[7] Crocetto F, Ferro M, Buonerba C, et al. Comparing cardiovascular adverse events in cancer patients: a meta-analysis of combination

therapy with angiogenesis inhibitors and immune checkpoint inhibitors versus angiogenesis inhibitors alone[J]. Crit Rev Oncol Hematol, 2023, 188: 104059.

[8] Sahoo D, Deb P, Basu T, et al. Advancements in platinum-based anticancer drug development: a comprehensive review of strategies, discoveries, and future perspectives[J]. Bioorg Med Chem, 2024, 112: 117894.

[9] Frigo E, Tommasin L, Lippe G, et al. The haves and have-nots: the mitochondrial permeability transition pore across species[J]. Cells, 2023, 12(10): 1409.

[10] Shen X, Ma M, Mi R, et al. EFHD1 promotes osteosarcoma proliferation and drug resistance by inhibiting the opening of the mitochondrial membrane permeability transition pore (mPTP) by binding to ANT3[J]. Cell Mol Life Sci, 2024, 81(1): 236.

[11] Zhao L, Tang M, Bode AM, et al. ANTs and cancer: Emerging pathogenesis, mechanisms, and perspectives[J]. Biochim Biophys Acta BBA Rev Cancer, 2021, 1875(1): 188485.

[12] Ji XZ, Chu LJ, Su D, et al. MRPL12-ANT3 interaction involves in acute kidney injury *via* regulating MPTP of tubular epithelial cells [J]. iScience, 2023, 26(5): 106656.

[13] Zhang JY, Wang M, Wang RY, et al. Salvianolic acid A ameliorates arsenic trioxide-induced cardiotoxicity through decreasing cardiac mitochondrial injury and promotes its anticancer activity[J]. Front Pharmacol, 2018, 9: 487.

[14] Feng AJ, Xu JK, Fu Y, et al. An integrative pharmacology-based study on the efficacy and mechanism of essential oil of Chaihu Guizhi Decoction on influenza A virus induced pneumonia in mice [J]. J Ethnopharmacol, 2025, 336: 118654.

[15] Wu L, Shen HY, Wu YZ, et al. Pharmacodynamics and potential synergistic effects of Mai-Luo-Ning injection on cardiovascular protection, based on molecular docking[J]. Chin J Nat Med, 2015, 13(11): 815-22.

[16] 黎卓涵, 王艳萍, 蔡娱飞. 中医药治疗卵巢癌及并发症的优势分析[J]. 吉林中医药, 2022, 42(12): 1469-72.

[17] Chen YL, Su R, Hu YG, et al. The active components and potential mechanisms of Li-Chong-Xiao-Zhen granules in the treatment of ovarian cancer: an integrated metabolomics, proteomics, network pharmacology and experimental validation[J]. J Ethnopharmacol, 2025, 343: 119474.

[18] Chen Y, Ma S, Pi D, et al. Luteolin induces pyroptosis in HT-29 cells by activating the Caspase1/Gasdermin D signalling pathway[J]. Front Pharmacol, 2022, 13: 952587.

[19] Lheureux S, Braunstein M, Oza AM. Epithelial ovarian cancer: Evolution of management in the era of precision medicine[J]. CA Cancer J Clin, 2019, 69(4): 280-304.

[20] Lai K, Chen Z, Lin S, et al. The IDH1-R132H mutation aggravates cisplatin-induced acute kidney injury by promoting ferroptosis through disrupting NDUFA1 and FSP1 interaction[J]. Cell Death Differ, 2025, 32(2): 242-55.

[21] Tang CY, Livingston MJ, Safirstein R, et al. Cisplatin nephrotoxicity: new insights and therapeutic implications[J]. Nat Rev Nephrol, 2023, 19(1): 53-72.

[22] Matulonis UA, Sood AK, Fallowfield L, et al. Ovarian cancer[J]. Nat Rev Dis Primers, 2016, 2: 16061.

[23] Colombo N, Sessa C, du Bois A, et al. ESMO-ESGO consensus conference recommendations on ovarian cancer: pathology and molecular biology, early and advanced stages, borderline tumours and recurrent disease[J]. Ann Oncol, 2019, 30(5): 672-705.

[24] 杨才志, 黄仲羽, 林洁涛, 等. 林丽珠治疗卵巢癌用药规律探讨[J]. 广州中医药大学学报, 2019, 36(12): 2027-33.

[25] 杨鹤年, 张津铖, 吴宿慧, 等. 中药配方颗粒制备工艺、质量评价、与传统汤剂一致性的研究现状分析[J]. 中国实验方剂学杂志, 2023, 29(8): 266-74.

[26] Halestrap AP, Richardson AP. The mitochondrial permeability transition: a current perspective on its identity and role in ischaemia/reperfusion injury[J]. J Mol Cell Cardiol, 2015, 78: 129-41.

[27] Pan TH, Yang B, Yao S, et al. Exploring the multifaceted role of adenosine nucleotide translocase 2 in cellular and disease processes: a comprehensive review[J]. Life Sci, 2024, 351: 122802.

[28] Liu G, Wang ZK, Wang ZY, et al. Mitochondrial permeability transition and its regulatory components are implicated in apoptosis of primary cultures of rat proximal tubular cells exposed to lead[J]. Arch Toxicol, 2016, 90(5): 1193-209.

[29] Kairys V, Baranauskiene L, Kazlauskiene M, et al. Recent advances in computational and experimental protein-ligand affinity determination techniques[J]. Expert Opin Drug Discov, 2024, 19 (6): 649-70.

[30] Lai H, Wang LY, Qian RY, et al. Interformer: an interaction-aware model for protein-ligand docking and affinity prediction[J]. Nat Commun, 2024, 15: 10223.

[31] Genin EC, Plutino M, Bannwarth S, et al. CHCHD10 mutations promote loss of mitochondrial cristae junctions with impaired mitochondrial genome maintenance and inhibition of apoptosis[J]. EMBO Mol Med, 2016, 8(1): 58-72.

[32] Martin-Solana E, Casado-Zueras L, Torres TE, et al. Disruption of the mitochondrial network in a mouse model of Huntington's disease visualized by in-tissue multiscale 3D electron microscopy[J]. Acta Neuropathol Commun, 2024, 12(1): 88.

[33] Li ZF, Feng JK, Zhao XC, et al. The extract of *Pinellia ternata*-induced apoptosis of leukemia cells by regulating the expression of bax, bcl-2 and caspase-3 protein expression in mice[J]. Transplant Proc, 2023, 55(9): 2232-40.

（编辑：余诗诗）